South China Sea hydrological changes and Pacific Walker Circulation variations over the last millennium

Hong Yan, Liguang Sun, Delia W. Oppo, Yuhong Wang, Zhonghui Liu, Zhouqing Xie, Xiaodong Liu, Wenhan Cheng

Supplementary Information

Supplementary Figures

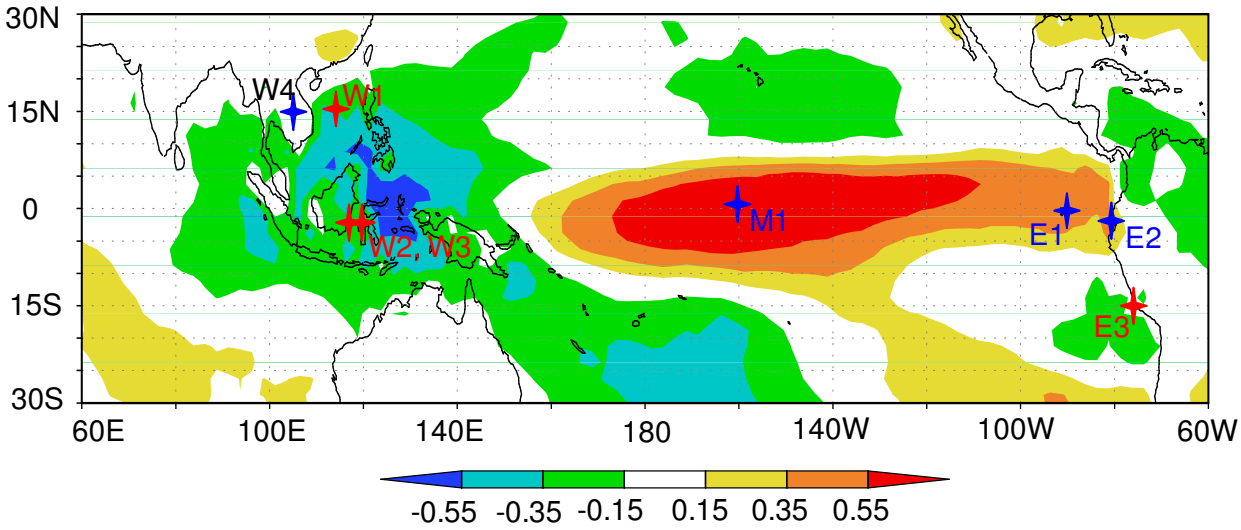

Supplementary Figure S1. Modern precipitation pattern of tropical Pacific. Correlations of monthly mean anomalies of precipitation[30] with the NINO3 index[31] from November 1981 to November 2010. Locations of hydrology records in the tropical Pacific are also indicated: W1-our South China Sea records, W2-Indonesia [6,7], W3-Indonesia[8], W4-Vietnam[20], M1-Washington Island[17], E1-Galapagos[13], E2-Ecuador[12] and E3-Peru[10,11]. Locations that were drier/wetter during the Little Ice Age than during the Medieval Climate Anomaly Period are marked in blue/red.

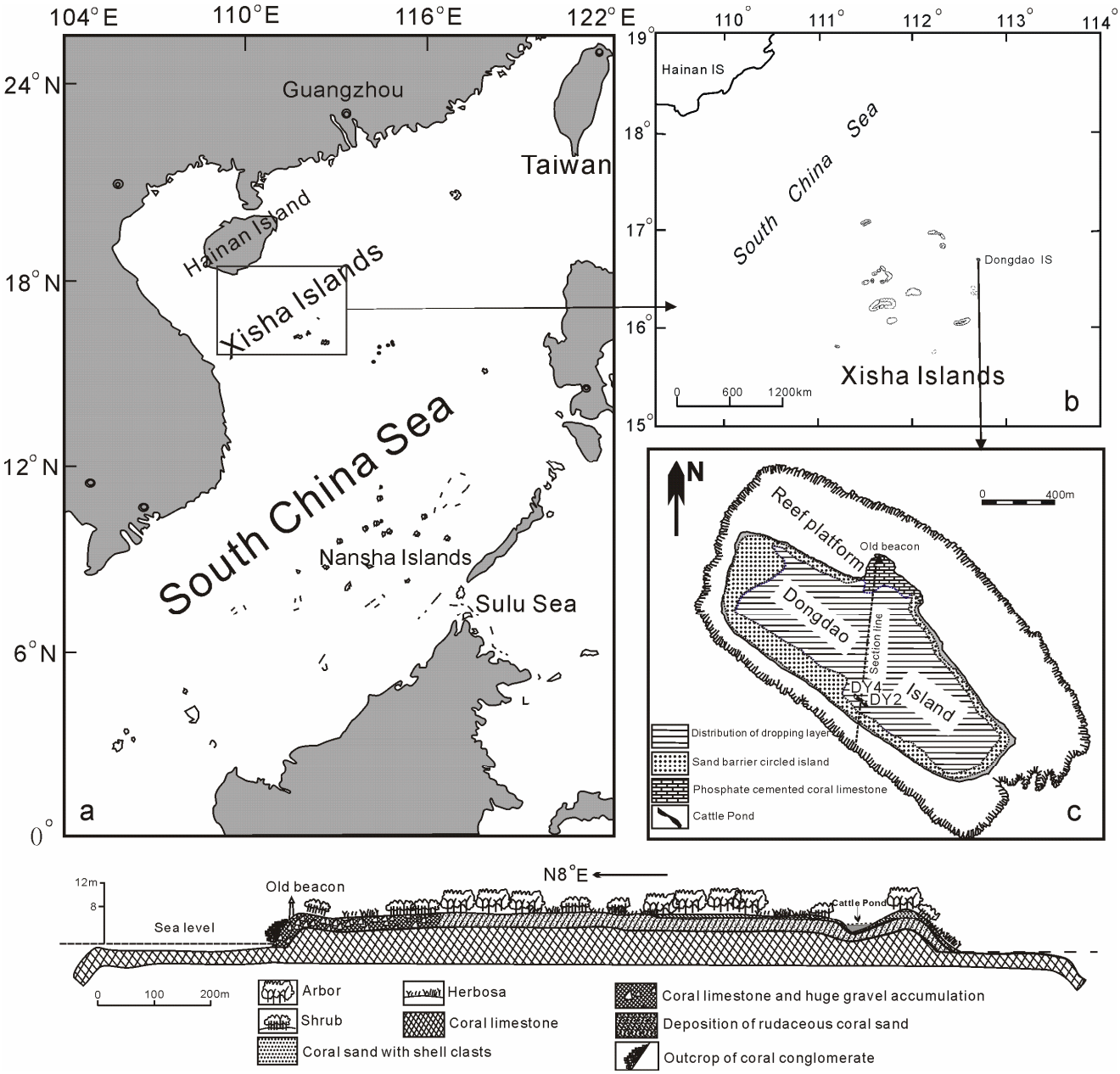

Supplementary Figure S2. Study area. Maps showing the geographical location of the study area (a), the Xisha Islands (b), the Dongdao Island (c), and the distribution of morphological zones of the Dongdao Island. The bottom diagram is the section drawing of topography, vegetations, soils and parent materials along the section line from old beacon to Cattle Pond, which is indicated in the top right figure (c).

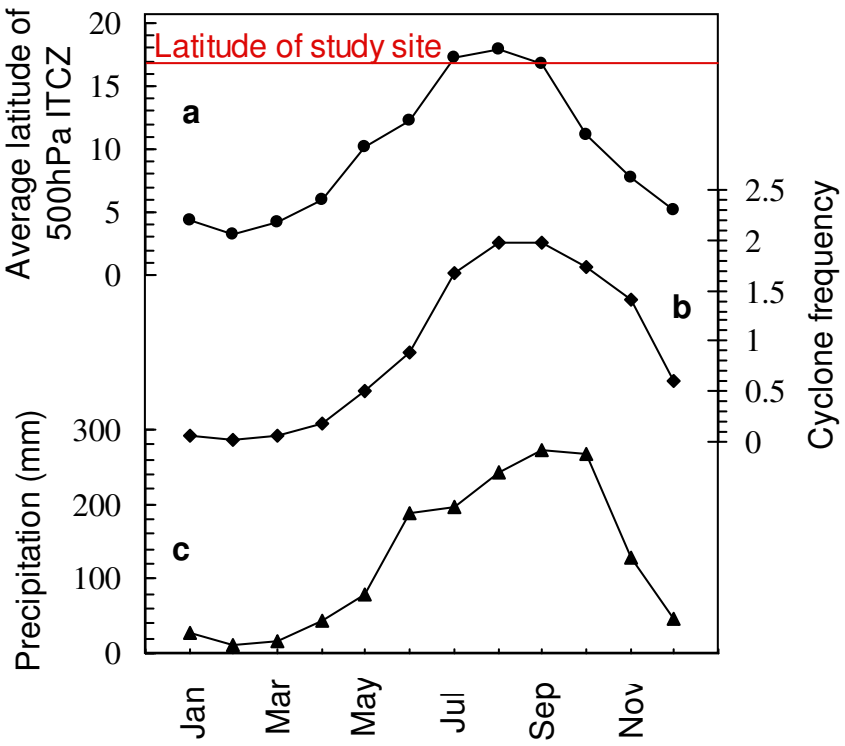

Supplementary Figure S3. Modern seasonal climatic characteristics in South China Sea. Monthly mean latitude of ITCZ in South China Sea from 1991 to 2001 (a)[14]. The red line indicates the latitude of our study site. Monthly mean cyclone frequency (b) and precipitation (c) in Dongdao Island from 1991 to 2001[14].

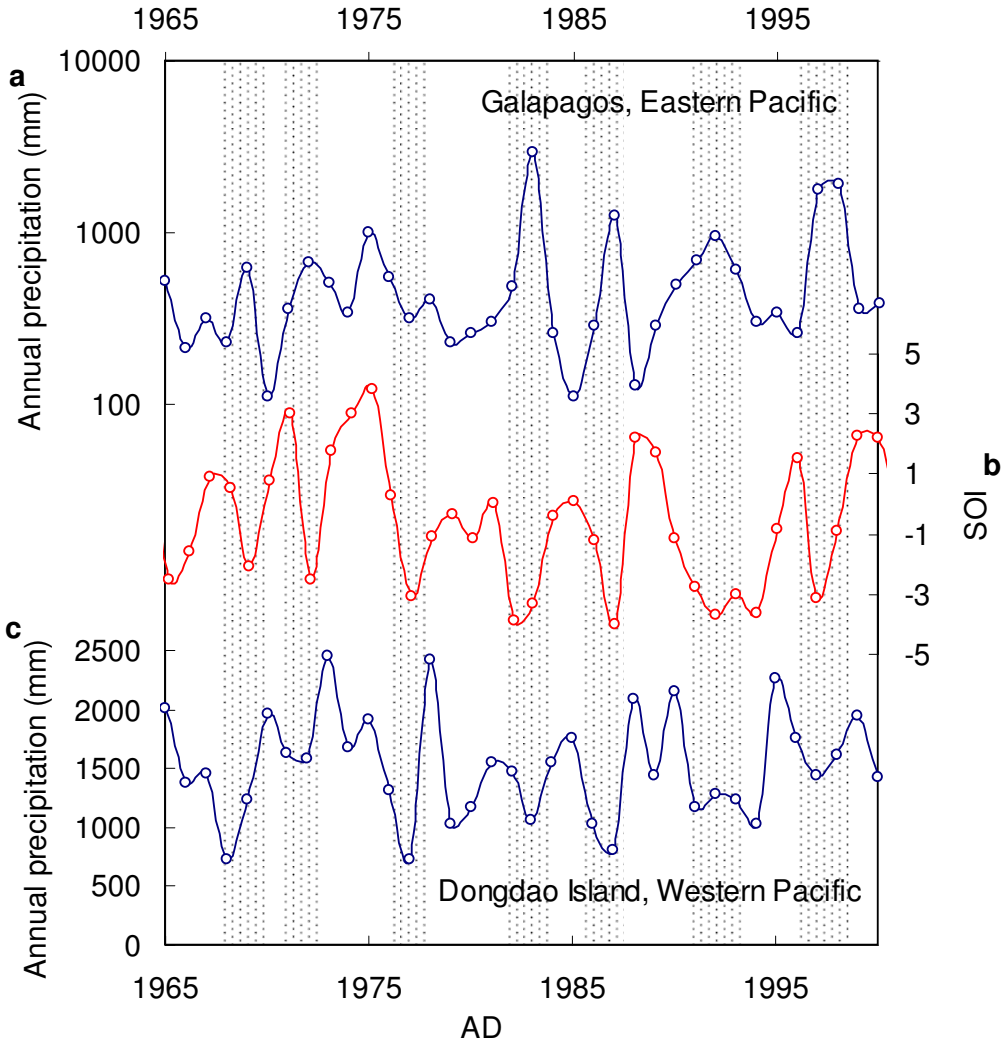

Supplementary Figure S4. Correlations between annual Southern Oscillation index and rainfall in Dongdao Island and Gálapagos. Comparisons of Gálapagos annual rainfall (a)[13], the SOI index (b)[16] and the annual rainfall on the Dongdao Island (c) during the period of 1965 to 2000. Gray bars represent El Niño events during this period. Precipitation changes in the western and eastern tropical Pacific exhibit a "seesaw effect" in response to the Pacific walker circulation variation, and the Gálapagos (Dongdao) annual rainfall from 1951 to 1997 (from 1958 to 2005) is negatively (positively) correlated with the SOI index, with $r=-0.43$, $p<0.005$, $n=47$ ($r=0.4$, $p<0.005$, $n=48$).

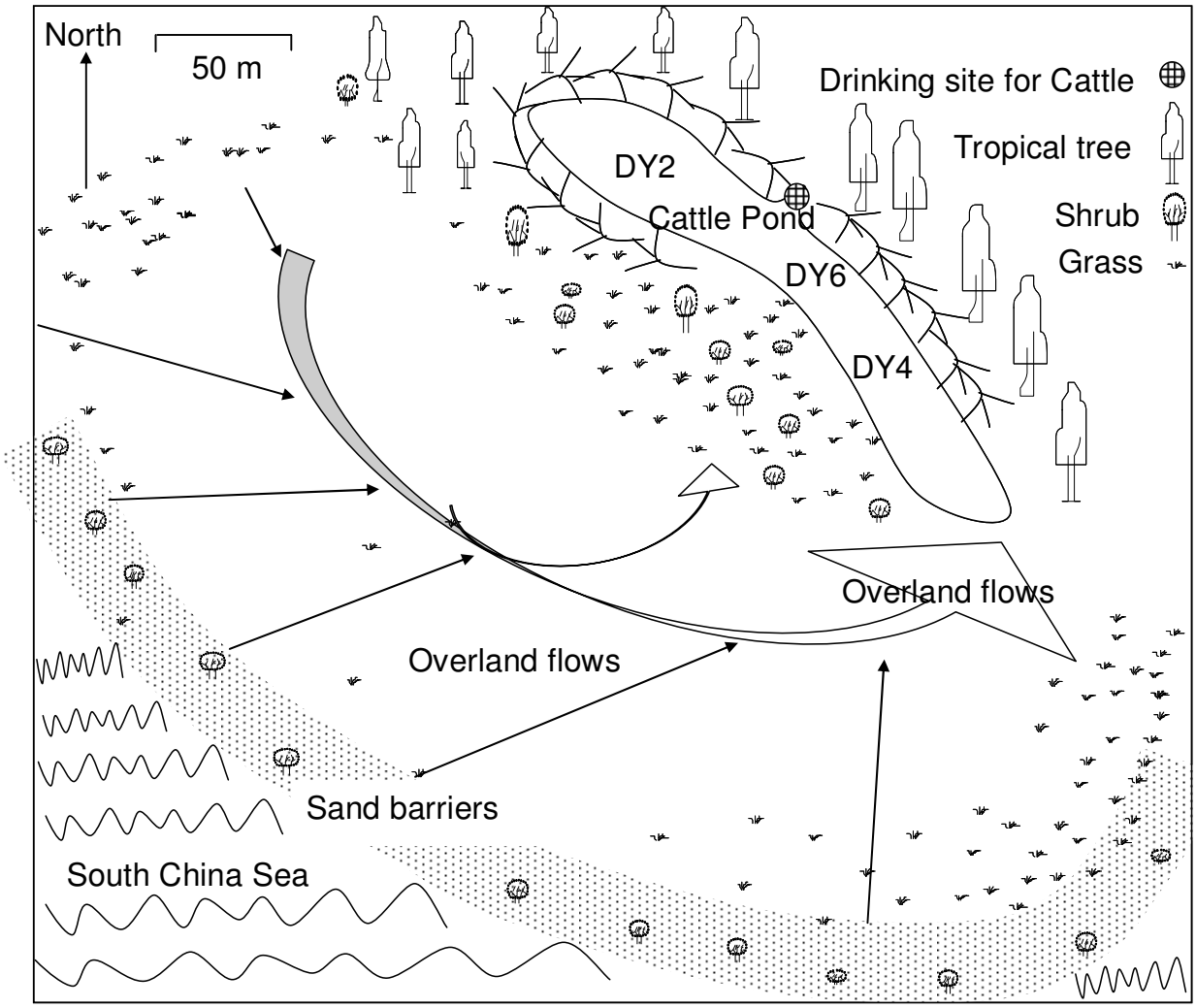

Supplementary Figure S5. Sampling site description. The geographical features of the "Cattle Pond". There are several dozens of cattle, which were brought to island in recent years, living in the centre woodland of the island. One might think this would disturb lake sediment. However, according to the investigation in the field, as well as in the laboratory, no disturbance is evident. First, the cattle on Dongdao Island are a variety of the Chinese yellow cattle that rarely wallow in water and mud. Second, we investigated their lifestyle over a month and found that the cattle lived in the centre island and never went out of the woodland. They drink water in only one small region of Cattle Pond where water trickles out into the woodland and is not barricaded by coral rocks. Third, our sampling sites are far away from the drinking corner and surrounded by coral rock. Combined with the progressive sedimentary lithology, similar sediment grain size variation of two cores and the results of ^{14}C dating, the disturbance from cattle does not seem to occur or is insignificant in the Cattle Pond.

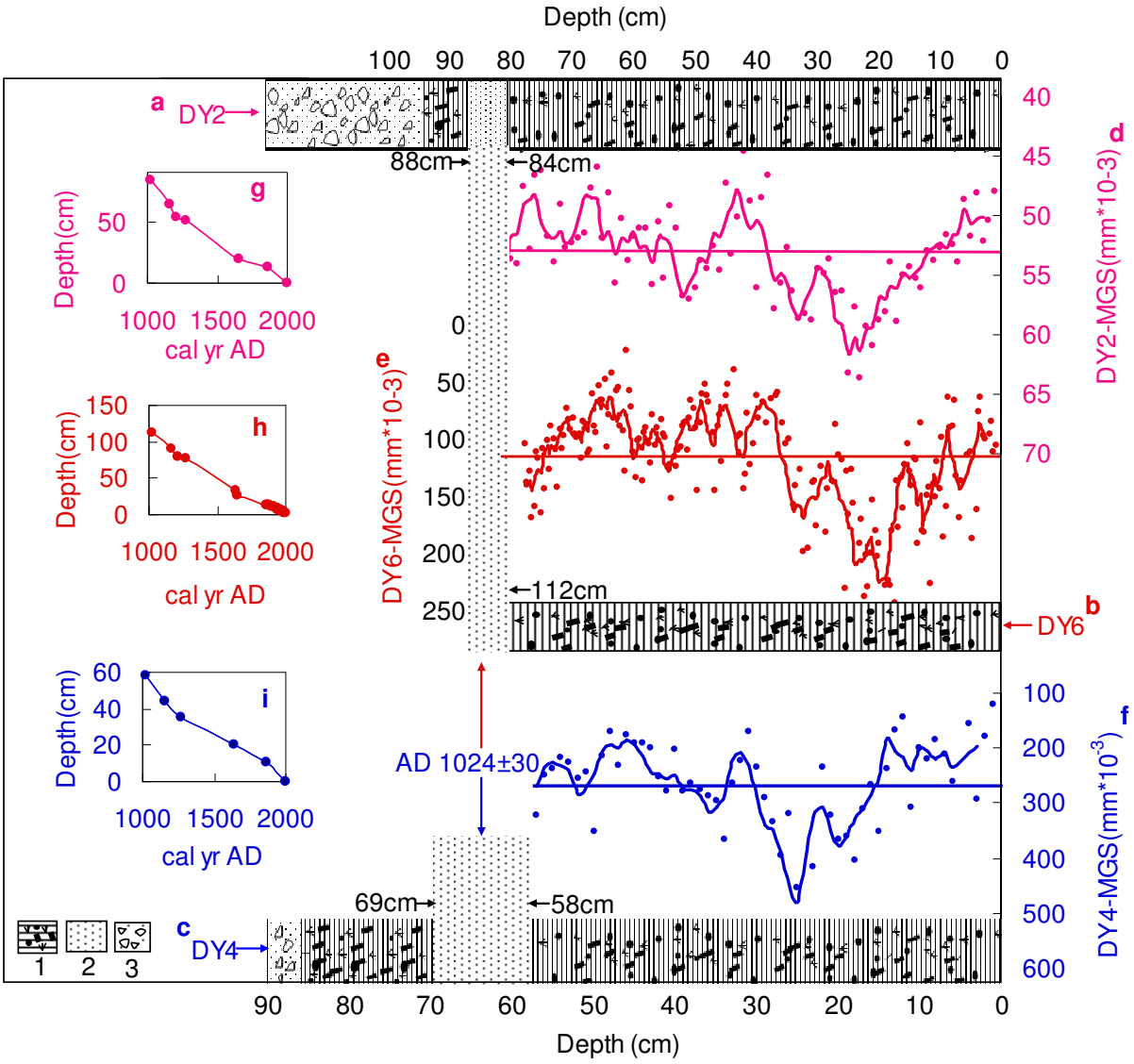

Supplementary Figure S6. Lithological characteristics of the lake sediment cores. Legend (left corner): 1. Middle to fine grained coral sandy mud with brown-red color, containing some plant remains and seabird droppings. 2. Well-sorted coral sand. 3. Grey-white coral, shell, and sandy gravel. A more detailed description of the lithological characteristics of DY2 and DY4 was given by Liu et al (2008)[18]. The similar fluctuations of sediment mean grain size (MGS)-versus-depth profiles (Original data and 3-point sliding standardized means) of DY2 core (d), DY6 (e) and DY4 (f) suggest that the sediments in the Cattle Pond have not been disturbed during or after deposition. This is further supported by the radiocarbon dating results, which show no age inversions with increasing depth. The radiocarbon dating of terrestrial plant remains in lake water body is not subjected to reservoir effects. Based upon the similar fluctuations of grain size profiles, the dating results of DY2, DY4 and DY6 correspond with each other and the age model of DY6 can be built from those of DY2 and DY4. The age for the surface sediment was assumed AD 2003, and the age between two adjacent dating results was obtained by linear interpolation. The age models are given in panels g, h, and i.

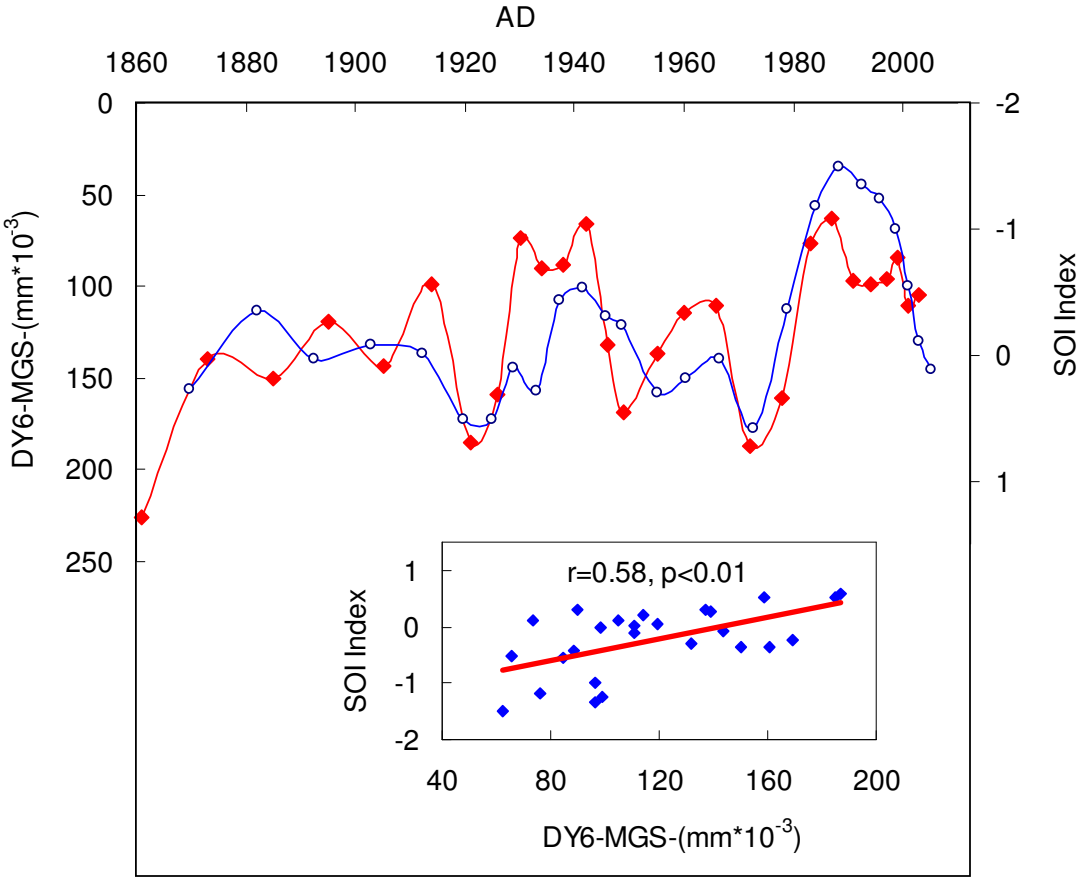

Supplementary Figure S7. Correlation between sediment grain size and SOI. Correlation between the DY6 sediment mean grain size and 10 year-smoothing instrumental Southern Oscillation Index (SOI)[15,16] over the last 140 years, time series comparison and scatter plot (r=0.58, p<0.01, n=26). SOI data come from http://www.cgd.ucar.edu/cas/catalog/climind/SOI.signal.annstd.ascii.

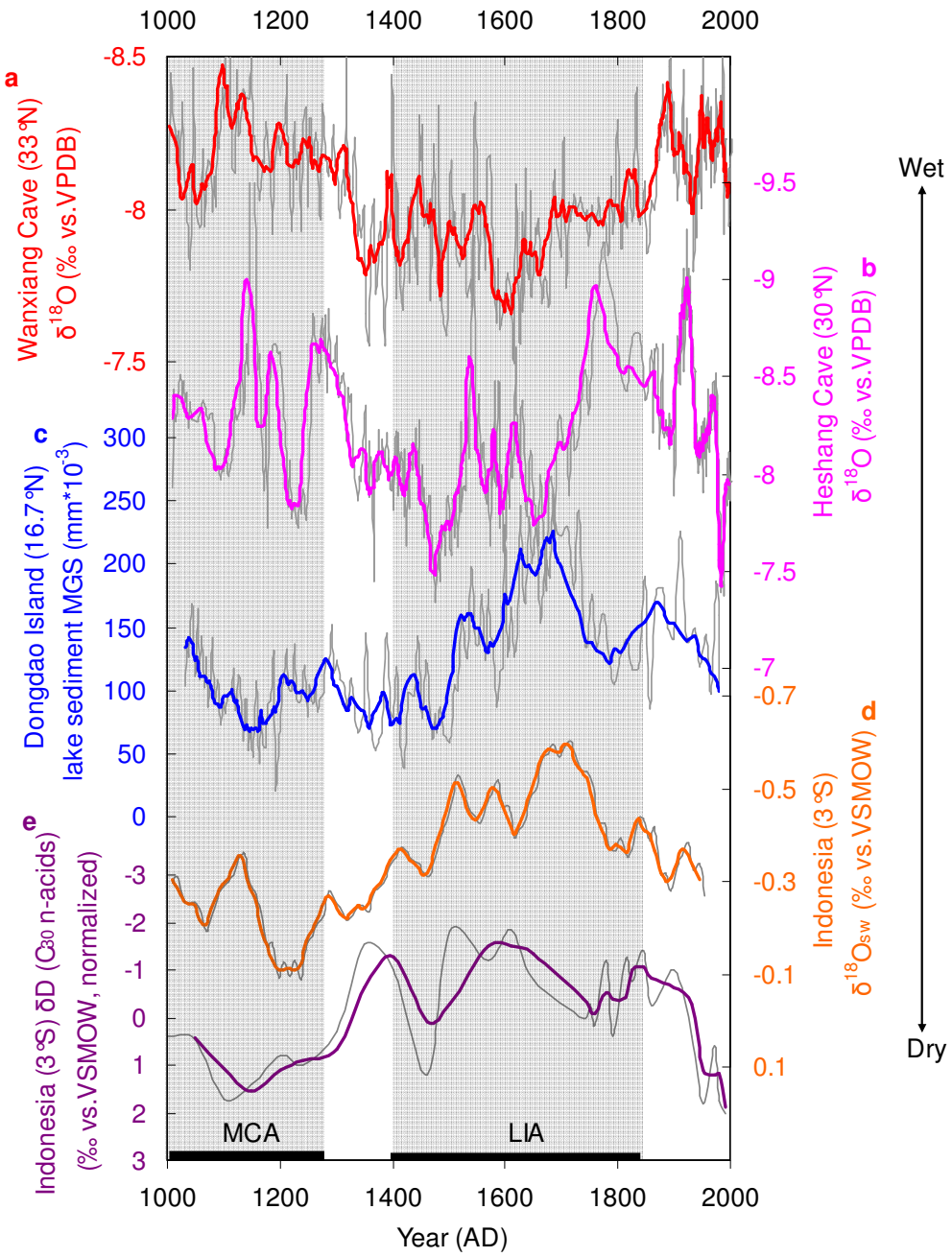

Supplementary Figure S8. Comparison with other Asia-western Pacific hydrological records. (a) $\delta^{18}O$ data from a Wanxiang Cave speleothem (raw data in gray and 6 point moving average in red)[5]; (b) $\delta^{18}O$ data from a Heshang Cave speleothem (raw data in gray and 6 point moving average in pink)[4]; (c) sediment grain size-versus-age profiles (DY6) of Cattle Pond (raw data in gray and 6 point moving average in blue, this study); (d) $\delta^{18}O_{sw}$ data from Indonesia marine sediment (raw data in gray and 2 point moving average in black)[7]; (e) Normalized δD_{wax} data from Indonesia marine sediment for the C_{30} *n*-acids (raw data in gray and 2 point moving average in purple)[8]; Gray bars represent the time periods of MCA (~ AD 800-1300) and LIA (~ AD 1400-1850).

Supplementary Tables

Laboratory number	Sample number	Dated material	Depth (cm)	^{14}C Conventional age (yr BP)	Calibrated age (cal yr BP)	
					Intercept	2 sigma
BA05842	DY4-21	Plant caryopsis	20-21	305±40	417, 314, 411	474-289
BA05843	DY4-36	Plant caryopsis	35-36	765±35	675	735-656
BA05844	DY4-45	Plant caryopsis	44-45	900±35	790	924-730
BA051074	DY4-58(1)	Plant caryopsis	57-58	1020±30	932	970-804
BA051075	DY4-58(2)	Plant caryopsis	57-58	985±30	926	953-794
BA051076	DY4-58(3)	Plant caryopsis	57-58	980±30	925	951-793
BA051077	DY4-71(1)	Plant caryopsis	70-71	1025±30	933	971-917
BA051078	DY4-71(2)	Plant caryopsis	70-71	960±30	916	945-790
BA051079	DY4-71(3)	Plant caryopsis	70-71	1010±40	930	972-795
BA051080	DY4-71(4)	Plant caryopsis	70-71	965±30	919	947-790
BA05846	DY4-71(5)	Plant caryopsis	70-71	995±35	928	966-794
BA05849	DY4-87	Plant caryopsis	86-87	1340±35	1284	1306-1181
BA03236	DY2-20	Bulk organic carbon	19-20	250±70	298	475-1
BA03237	DY2-54	Bulk organic carbon	53-54	850±60	738	923-667
BA03239	DY2-95	Bulk organic carbon	94.5	1440±65	1327	1510-1262
BA03240	DY2-C1	Plant caryopsis	94.5	1360±40	1288	1331-1184

Supplementary Table S1. AMS ^{14}C dating results. AMS ^{14}C dates and calibrated ages of the sediment cores from the Cattle Pond on the Dongdao Island

Depth (cm)	^{210}Pb activity (dpm/g)(±4)	Cum.dry mass (g/cm^2)	Modeled age (yr AD)
0.25	197.754	0.38	2003
0.75	210.832	0.715	2001
1.25	174.692	1.095	1999
1.75	192.015	1.575	1997
2.25	164.671	2.085	1994
2.75	193.251	2.605	1991
3.25	170.714	3.125	1987
3.75	182.171	3.655	1983
4.25	174.539	4.215	1978
4.75	165.618	4.705	1972
5.25	129.575	5.225	1966
5.75	94.653	5.725	1960
6.25	90.397	6.255	1955
6.75	38.544	6.795	1949
7.25	51.885	7.275	1946
7.75	44.001	7.775	1942
8.25	45.197	8.205	1938
8.75	34.337	8.705	1934
9.25	32.268	9.175	1930
9.75	32.344	9.685	1926
10.25	35.541	10.225	1921
10.75	35.056	10.775	1914
11.25	32.592	11.265	1905
11.75	20.916	11.825	1895
12.25	18.541	12.365	1885
12.75	13.273	12.885	1873
13.25	26.407	13.465	1861

Supplementary Table S2. ^{210}Pb dating results. ^{210}Pb activity (unsupported), cumulative dry mass and modeled ages of DY6. The ^{210}Pb chronology was constructed by assuming constant rate of supply (CRS) and relating the exponential ^{210}Pb decay profiles with the cumulative dry mass – depth profiles as determined using bulk density measurements (DY6) and using a CRS computer model. dpm/g = decays per minute per gram dry sediment[17].

Supplementary References

[30] Janowiak, J. E. & Xie, P. P. CAMS-OPI: A global satellite-rain gauge merged product for real-time precipitation monitoring applications. *Journal of Climate* **12**, 3335-3342 (1999).

[31] Reynolds, R. W., Rayner, N. A., Smith, T. M., Stokes, D. C. & Wang, W. Q. An improved in situ and satellite SST analysis for climate. *Journal of Climate* **15**, 1609-1625 (2002).